Acta Crystallographica Section D
Biological Crystallography
ISSN 0907-4449

Critical importance of loop conformation to avidin-enhanced hydrolysis of an active biotin ester

Ruchama Hayouka,[a] Yael Eisenberg-Domovich,[a] Vesa P. Hytönen,[b] Juha A. E. Määttä,[b] Henri R. Nordlund,[b] Markku S. Kulomaa,[b] Meir Wilchek,[a] Edward A. Bayer[a] and Oded Livnah[a]*

[a]Department of Biological Chemistry, The Institute of Life Sciences, The Wolfson Centre for Applied Structural Biology, The Hebrew University of Jerusalem, Givat Ram, Jerusalem 91904, Israel, and [b]Institute of Medical Technology, FI-33014 University of Tampere, Tampere, Finland

Correspondence e-mail: oded.livnah@huji.ac.il

Received 22 November 2007
Accepted 20 December 2007

PDB References: apo AVR4(D39A), 2of8, r2of8sf; AVR4(D39A)–BNA complex, 2of9, r2of9sf; apo AVR4(R112L), 2ofa, r2ofasf; AVR4(R112L)–BNA complex, 2ofb, r2ofbsf.

The homotetrameric and biotin-binding properties of avidin and streptavidin have been exploited for a myriad of biotechnological applications and theoretical studies. Among the few differences between the two proteins is the capacity of avidin to hydrolyze biotinyl *p*-nitrophenyl ester (BNP), as opposed to streptavidin, which fully protects the same pseudosubstrate from hydrolysis. Combined mutagenesis and X-ray analysis have been used to attempt to understand this diametric difference in activities. It was found that a charged residue and one of the loops (L3,4) are together responsible for this difference. Recently, the avidin-related analogue AVR4 was found to have an even more pronounced BNP-hydrolysis activity than avidin. Again, the combination of charged residue(s) (Asp39 and/or Arg112) and the rigid conformation of the L3,4 loop was suggested to be responsible for the observed hydrolysis reaction. However, replacement of the latter charged residues in AVR4 resulted in only a modest reduction in hydrolytic activity at most, whereas replacement of the L3,4 loop of avidin with the rigid loop of AVR4 caused a dramatic increase in the activity of avidin. These results clearly demonstrate that the main feature responsible for the observed differences in rates of hydrolysis among the avidins is the conformational status of the L3,4 loop, which imposes conformational constraints on the pseudosubstrate, thereby rendering it susceptible to nucleophilic attack by solvent. In this context, the hydrolytic properties of the avidins reflect enzyme catalysis, in that subtleties in substrate binding are the determining features of catalytic efficiency.

1. Introduction

Chicken avidin and its bacterial analogue streptavidin are high-affinity biotin-binding proteins that share many structural and chemical properties (Green, 1975, 1990). Both proteins are homotetrameric with a single biotin-binding site per subunit. Their high affinities towards biotin have been extensively exploited in a variety of biotechnological and nanotechnological applications (Wilchek & Bayer, 1990; Grubmuller, 2005; Amemiya *et al.*, 2005).

In recent work (Huberman *et al.*, 2001), the hydrolytic enhancement of biotinyl *p*-nitrophenyl ester (BNP) has been demonstrated, in which avidin displays an intriguing pseudo-catalytic capacity, in contrast to the protection of the active ester by streptavidin. In this particular characteristic, the two proteins differ completely.

The factors that dictate the differences in the pseudo-catalytic properties were deduced *via* structural analysis of the proteins in complex with biotinyl *p*-nitrophenyl anilide (BNA), an inert amide analogue of BNP (Huberman *et al.*, 2001). Two main factors were found to promote hydrolysis in avidin: (i) disorder of the L3,4 loop (connecting the β3 and β4 strands), which renders the BNP ester bond accessible to nucleophilic attack, and (ii) interaction of the ligand with the ε-amino group of Lys111 from an adjacent monomer, which serves to increase the leaving-group propensity of the *p*-nitrophenyl moiety. In streptavidin the L3,4 loop is three residues shorter than that in avidin and exhibits a closed conformation upon ligand binding. The involvement of the latter two molecular features was further verified by site-directed mutagenesis of streptavidin, which served to convert the protein from a protector of the BNP ligand into an enhancer (like avidin) of its hydrolysis (Pazy, Raboy *et al.*, 2003; Eisenberg-Domovich *et al.*, 2004). In addition, the role of Lys111 in avidin was verified by the reduced hydrolytic activity of the K111I mutant (Prizant *et al.*, 2006).

In addition to avidin, the chicken genome contains a family of seven avidin-related genes that exhibit high homology to the avidin sequence (Keinanen *et al.*, 1994; Hytönen *et al.*, 2005). Genes AVR1–AVR7 have been used to express functional recombinant proteins capable of biotin binding (Laitinen *et al.*, 2002). One of these gene products, AVR4 (and its translation equivalent AVR5), exhibits near-identical tertiary and quaternary structures to those of avidin and streptavidin and shares the extremely high binding affinity towards biotin (Kurzban *et al.*, 1991; Eisenberg-Domovich *et al.*, 2005; Green, 1975, 1990). The tetrameric structure of the avidins is essential for their high biotin-binding affinity, in which a tryptophan residue is donated from an adjacent subunit to each biotin-binding site, thus contributing both to the binding affinity and to the integrity of the tetramer (Sano & Cantor, 1995; Chilkoti *et al.*, 1995).

Recently, it was discovered that AVR4 displays an extraordinary pseudo-catalytic activity that far exceeds that of avidin (Prizant *et al.*, 2006). Analysis of the high-resolution crystal structure of the AVR4–BNA complex (Prizant *et al.*, 2006) led us to propose several factors that promote the extraordinary AVR4-mediated hydrolysis of BNP (Eisenberg-Domovich *et al.*, 2005; Prizant *et al.*, 2006). The L3,4 loops in both avidin and AVR4 have the same length (as opposed to that of streptavidin) yet differ in amino-acid composition. The L3,4 loop in avidin is highly flexible (Livnah *et al.*, 1993; Pazy *et al.*, 2002), whereas in AVR4 the loop includes a distinctive Pro-Gly that exhibits a rigid conformation (Prizant *et al.*, 2006; Eisenberg-Domovich *et al.*, 2005). In the apo and biotin-complexed AVR4 the L3,4 loop is further stabilized by a salt-bridge interaction between Asp39 and Arg112 (Prizant *et al.*, 2006). Upon BNA binding, the salt-bridge interaction is disrupted by the presence of the *p*-nitroanilide moiety. Consequently, the original salt-bridge partners now form two major polar interactions with the BNA: (i) Asp39 of the L3,4 loop forms hydrogen-bond interactions with one of the BNA nitro O atoms and with Lys109 (equivalent to Lys111 in avidin) from the adjacent monomer and (ii) Arg112 (strand β8) forms π–cation and hydrogen-bond interactions with the *p*-nitroanilide group of the ligand. These observations suggest that Asp39 may play a role in promoting the hydrolytic reaction and, more importantly, that Arg112 may serve as the major electron-withdrawing entity in AVR4 as opposed to Lys111 in avidin. Indeed, the AVR4 K109I mutant exhibits much higher activity towards BNP than the wild-type avidin. Taken together, these results suggest an alternative compensating reaction mechanism for AVR4 in the hydrolysis of BNP. Based on the previous observations, it became clear that the L3,4 loop and the charged amino acids that interact with the BNP nitro group play a combined role in enhancing hydrolysis.

In this study, the factors proposed to promote the exceptional hydrolytic activity of AVR4 were examined further by loop replacement and site-directed mutagenesis. For this purpose, the L3,4 loop of avidin was replaced by the rigid Pro-Gly-containing loop of AVR4 [denoted as avidin(L3,4-AVR4)] and the resultant mutant exhibited heightened hydrolytic activity. The results clearly demonstrated that the L3,4 loop in AVR4 plays a substantial role in promoting BNP hydrolysis. In addition, the crystal structures of the R112L and D39A mutants of AVR4 were elucidated, which revealed a critical role for Arg112 in BNP hydrolysis but virtually no role for Asp39.

2. Materials and methods

As defined previously (Eisenberg-Domovich *et al.*, 2005), the AVR4 derivative and all its corresponding variants represent the C122S mutant, which displays near-identical properties to the wild-type protein and will henceforth be referred to as AVR4 (Hytönen, Laitinen *et al.*, 2004).

2.1. Expression and purification of AVR4(D39A), AVR4(R112L) and avidin(L3,4-AVR4)

The DNA constructs previously used in the expression of avidin (Hytönen, Laitinen *et al.*, 2004) and AVR4 (Hytönen *et al.*, 2005) were used as a starting point in this study. These DNA constructs, each of which contained *attL* homologous recombination sites and a sequence encoding the signal peptide from bacterial OmpA protein, were subjected to QuikChange mutagenesis in pGEMTeasy plasmid in order to introduce the D39A and R112L mutations into AVR4. The rationale for the mutagenesis came from sequence analysis of biotin-binding proteins, such that Arg112 in AVR4 was replaced by the Leu found in streptavidin and Asp39 in AVR4 was replaced by the Ala from chicken avidin, according to multiple sequence alignment (not shown). To replace the region corresponding to L3,4 in avidin by the analogous region from AVR4, consecutive PCR reactions were carried out, in the first of which L3,4 from avidin cDNA was extracted with primers having avidin-specific overhanging regions. A second reaction was used to extract the N-terminal *attL* site and the DNA encoding the signal peptide together with the N-term-

inal portion of the avidin sequence; the product was then combined with the first reaction product by a third PCR, which employed homologous regions at the DNA termini. The fourth PCR extracted the other *attL* site and DNA encoding the C-terminal portion of avidin; the product was combined with that of the third reaction by a fifth PCR that included homologous regions of the DNA termini. All the constructs were then subcloned into the pBVboostFG expression vector (Laitinen *et al.*, 2005) using the LR cloning reaction (Invitrogen) and were verified by DNA sequencing. The *Escherichia coli* BL21-AI cell line (Invitrogen) was used for expression and 2-iminobiotin agarose (Affiland S.A., Ans-Liege, Belgium) affinity chromatography was used for protein isolation and purification as described previously (Hytönen, Nyholm *et al.*, 2004). The proteins produced were subjected to analytical gel filtration using a Superdex HR10/30 column (Amersham) with 50 m*M* sodium phosphate with 650 m*M* NaCl pH 7.0 in the liquid phase. The analysis was carried out essentially as described previously (Hytönen *et al.*, 2003).

2.2. Hydrolysis assay

3.5 nmol BNP (Sigma B5383) was dissolved in 1 µl dimethylformamide and the solution was added to a solution (8 nmol in 50 µl 0.1 *M* sodium acetate pH 4) of avidin, AVR4 or the desired mutant. The molar ratio does not permit the availability of free BNP in solution. The solution was vortexed and incubated for 5–10 min at room temperature. After incubation, the protein solution was added to a 96-well microtitre plate. The pH was adjusted to the desired value (pH 6.5–9.5) by adding the appropriate phosphate buffer (200 µl, 0.1 *M*), which was calibrated as described previously (Pazy *et al.*, 2003; Prizant *et al.*, 2006). Hydrolysis of free BNP was used as a control. The progression and extent of the hydrolysis reaction was monitored by the release of *p*-nitrophenol at A_{405} as a function of time and pH using a plate reader (GENios Reader; Tecan, Mannedorf, Switzerland).

2.3. Crystallization and data collection

Crystals of the apo AVR4 variants were obtained by the hanging-drop vapour-diffusion method under similar crystallization conditions to those reported previously (1.5–1.9 *M* sodium formate, 0.1 *M* acetate buffer pH 4.2–4.6; Prizant *et al.*, 2006; Eisenberg-Domovich *et al.*, 2005). Diamond-shaped crystals grew after several hours and reached a final size of 0.4–0.6 mm after 7–14 d. Crystals of the respective BNA complexes were obtained by cocrystallization. BNA, a stable amide analogue of BNP, was dissolved in DMF and added to the protein solution (<1% volume). The solution was then incubated at room temperature for 20 h. Complex formation was monitored using the azo dye HABA as described previously (Livnah *et al.*, 1993; Huberman *et al.*, 2001). Crystals of the AVR4(R112L)–BNA and AVR4(D39A)–BNA complexes were obtained as described above for the apo forms. In cases where these conditions failed to result in spontaneous crystal growth, we applied the streak-seeding technique (Stura & Wilson, 1991). Diamond-shaped crystals (similar to those of the apo forms) were obtained after 24–48 h and usually reached a size suitable for X-ray analysis after several days. Prior to data collection, crystals were suspended in a cryoprotectant solution containing 25% glycerol and reservoir solution. Crystallographic data for all mutants were collected at 100 K using an Oxford Cryosystems Cryostream cooling device at The European Synchrotron Radiation Facility (ESRF), Grenoble, France. All of the crystals (similar to those of the wild-type AVR4) belonged to the tetragonal space group $P4_12_12$ with two monomers in the asymmetric unit (Table 1). All data were processed and scaled using the *HKL* suite (Otwinowski & Minor, 1997).

3. Results

3.1. Characteristics of the modified proteins

The expression and purification of the modified proteins was efficient and the yields after purification (~2–10 mg protein per litre of culture medium) were typical for avidin and AVR4 (Hytönen, Laitinen *et al.*, 2004). Gel-filtration analysis showed homogeneity of the samples and revealed a tetrameric quaternary structure for all proteins. The elution times were 30.2–30.5 min and the calculated molecular weights were 43–46 kDa. The low values observed for the molecular weight by gel-filtration analysis compared with the theoretical weights of the protein tetramers (56.4–57.4 kDa) are typical for avidin and AVR4 and possibly result from their high positive charge at pH 7.

3.2. BNP hydrolysis by avidins

The hydrolysis profiles of the AVR4 mutants R112L and D39A and avidin(L3,4-AVR4) were compared with those of wild-type AVR4, avidin and free BNP at pH values ranging from 6.5 to 10.0. No significant difference was observed for AVR4(D39A) compared with wild-type AVR4 (Fig. 1); the D39A mutant showed complete hydrolysis at pH 8.0 after less than 2 min of reaction (not shown). It thus appears that despite the hydrogen-bonding interaction with BNA, Asp39 in AVR4 has little if any effect on the enhancement of the reaction. On the other hand, the R112L mutation appears to play a more dramatic role in the reaction. After 10 min of reaction at pH 7.0, AVR4(R112L) had completed only 40% of the hydrolysis reaction compared with 90% for the wild-type protein (Fig. 1*b*). In this case, full hydrolysis is only reached at pH 8.0. Although the R112L mutant displays significantly weaker activity than wild-type AVR4, it is still much more potent than avidin (Fig. 1). These results clearly substantiate the role of Arg112 in enhancing the hydrolytic reaction, in which the interaction of Arg112 with the nitro group of BNP withdraws electrons, thus increasing the leaving-group propensity of *p*-nitrophenol.

Replacement of the L3,4 loop in avidin with that of AVR4 had a striking effect on the hydrolysis of BNP (Fig. 1). By grafting the AVR4 loop into avidin, the resultant hydrolysis reached approximately 60% after 10 min of reaction at pH 7.5, compared with 10% for avidin. At pH 8.5, avidin(L3,4-AVR4)

Table 1
Data-collection and refinement statistics.

Values in parentheses are for the outer resolution shell.

	AVR4(D39A)	AVR4(D39A)–BNA	AVR4(R112L)	AVR4(R112L)–BNA
ESRF beamline	ID29	ID14-4	ID14-3	ID14-4
Wavelength (Å)	0.9791	0.9253	0.9310	0.9253
Space group	$P4_12_12$	$P4_12_12$	$P4_12_12$	$P4_12_12$
Unit-cell parameters (Å)	a = 77.61, c = 110.48	a = 78.17, c = 110.29	a = 77.85, c = 110.78	a = 77.90, c = 110.33
Resolution range (Å)	63.25–1.35 (1.4–1.35)	63.25–1.05 (1.09–1.05)	63.25–1.50 (1.53–1.50)	40.0–1.16 (1.2–1.16)
Unique reflections	88271	150801	55076	142049
Redundancy	6.5	11.3	7.1	5.0
$R_{\rm merge}(I)$† (%)	3.8 (59.7)	6.2 (59.8)	4.6 (48.7)	5.6 (67.3)
Completeness (%)	98.8 (89.6)	100.0 (100.0)	99.8 (97.8)	95.1 (93.4)
$I/\sigma(I)$	38.2 (1.6)	47.5 (2.7)	25.0 (1.6)	37.0 (1.6)
No. of protein atoms	1891	1891	1882	1882
No. of ligand atoms	—	50	—	50
No. of solvent atoms	179	245	182	139
No. of formate atoms	45	33	24	27
R factor (%)	17.0	16.3	17.2	17.7
$R_{\rm free}$‡ (%)	19.2	17.2	18.8	18.7
Average B factor (Å^2)				
Protein	18.27	11.93	16.32	15.2
Ligand	—	14.25	—	15.2
Solvent	23.42	15.00	19.07	22.88
Formate	31.08	28.88	22.77	33.14
R.m.s.d. from ideality				
Bond lengths (Å)	0.012	0.010	0.016	0.011
Bond angles (°)	1.453	1.462	1.573	1.436
Ramachandran plot (%)				
Favoured	93.3	93.8	94.3	92.8
Allowed	6.7	6.2	5.7	6.2
Generously allowed	0	0	0	0
Disallowed	0	0	0	0

† $R_{\rm merge}(I) = \sum_{hkl}\sum_i |I_i(hkl) - \langle I(hkl)\rangle| / \sum_{hkl}\sum_i I_i(hkl)$. ‡ Test set consists of 5% of all data.

reaches maximal activity after less than 10 min of reaction (Fig. 1), whereas avidin requires approximately 10 h to reach complete hydrolysis (data not shown) (Huberman *et al.*, 2001; Pazy, Raboy *et al.*, 2003). Avidin(L3,4-AVR4) displays a similar reaction profile to that of AVR4(R112L) (Fig. 1), although in both cases the observed hydrolysis rate is still lower than that of AVR4.

3.3. Refinement of the apo forms and BNA complexes of the AVR4 mutants

The crystallographic data from the protein crystals revealed them to have identical symmetry and similar unit-cell parameters to those of the AVR4–BNA complex (Prizant *et al.*, 2006). A molecular-replacement protocol was thus not required for the structures and the models were directly refined as subsequently described.

The initial refinement model was the AVR4–BNA complex (PDB code 2fhl) after removing the ligand and solvent molecules. The model for the structure of the AVR4(R112L)–BNA complex was initially refined in the resolution range 10–4 Å using the rigid-body protocol in *REFMAC*5 (Murshudov *et al.*, 1997) as implemented in *CCP*4*i* (Potterton *et al.*, 2003) and was then further refined by restrained refinement in the resolution range 40–1.16 Å. The electron-density map clearly indicated the presence of the BNA ligand in the binding site as well as negative density for part of Arg112 (Fig. 2). This residue was altered to leucine, thus correcting the electron density in this area. The structure was built and fitted to electron-density maps using the program *O* (Jones & Kjeldgaard, 1997). Solvent molecules were added using *ARP*/*wARP* (Lamzin & Wilson, 1993). The other three structures were refined to the resolutions designated in Table 1 using a similar protocol to that described above. The final model of AVR4(D39A) consists of residues 3–122 for monomers 1 and 2 with 15 formate and 179 solvent molecules. The AVR4(D39A)–BNA complex consisted of residues 3–122 for monomers 1 and 2, with two BNA, 11 formate and 245 solvent molecules. The model of AVR4(R112L) consisted of residues 3–122 and 4–122 for monomers 1 and 2, respectively, eight formate and 182 solvent molecules. The model of the AVR4(R112L)–BNA complex consisted of residues 3–122 and 4–122 for monomers 1 and 2, respectively, with two BNA, nine formate and 136 solvent molecules (Table 1). The coordinates of the apo and BNA complexes of the D39A (PDB codes 2of9 and 2of8, respectively) and R112L (PDB codes 2ofa and 2ofb, respectively) mutants of AVR4 are available from the RCSB Protein Data Bank (Berman *et al.*, 2002).

3.4. The structures of AVR4(R112L) and AVR4(D39A)

The overall structures of the apo forms and BNA complexes of the AVR4 variants are similar to those observed for other avidins, with the tertiary structure consisting of eight antiparallel β-strands that form a β-barrel. The homotetrameric quaternary structure consists of a dimer of dimers, as described previously (Livnah *et al.*, 1993; Hendrickson *et al.*, 1989; Eisenberg-Domovich *et al.*, 2005; Kurzban *et al.*, 1991).

The apo structures of AVR4(D39A) and AVR4(R112L) are highly similar to the structure of wild-type AVR4. In the absence of biotin, the binding sites are occupied by two formate ions, which share similar positions in the three models, and 1–3 solvent molecules in conserved positions as also found in the apo AVR4 model (Eisenberg-Domovich *et al.*, 2005). The main notable difference between the three proteins is the status of the L3,4 loop (Fig. 3). In wild-type AVR4, Asp39 from the L3,4 loop forms a salt-bridge interaction with Arg112 from the β8 strand (Fig. 3*a*). Upon mutation of either of these

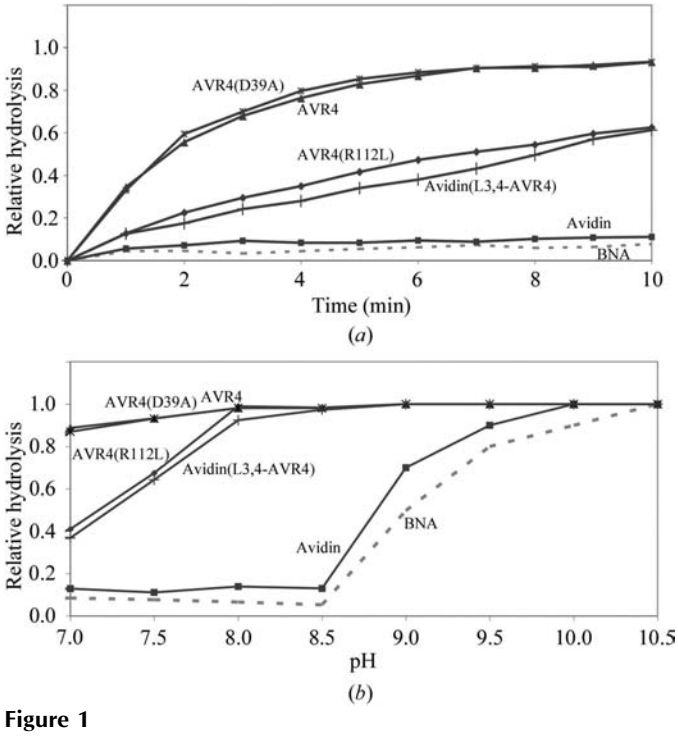

Figure 1
Hydrolytic activity of the various avidins. (*a*) Hydrolytic activity of the avidins in the initial 10 min of reaction with BNP at pH 7.5 compared with that of the free reagent (dashed line). The similar reaction profiles of wild-type AVR4 and its D39A mutant clearly indicate that Asp39 plays no role in enhancing the hydrolytic activity. Conversely, the R112L mutant results in a decrease in activity, emphasizing the role of the positively charged residue in the hydrolysis of BNP. The replacement of the L3,4 loop in avidin with that of AVR4 results in a dramatic increase in activity, demonstrating the role of this loop in the activity. Experiments were performed in triplicate and the error in absorption was ±3%. (*b*) Relative hydrolysis of BNP as a function of pH, monitored after 10 min of reaction. The graph clearly demonstrates the remarkable activity of avidin(L3,4-AVR4), which approaches that of wild-type AVR4 at pH 8.0, indicating its crucial role in enhancing BNP hydrolysis.

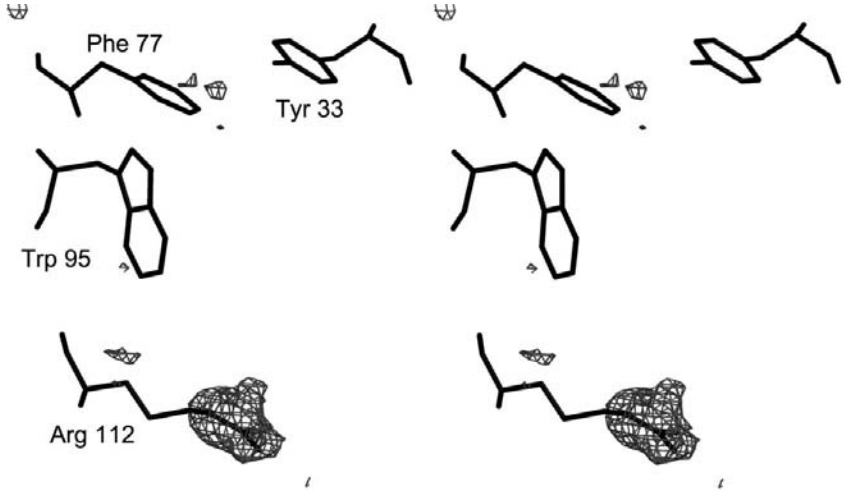

Figure 2
Electron-density map of the AVR4(R112L)–BNA complex. A stereoview of the negative difference electron-density map ($F_o - F_c$) calculated with data in the resolution range 40.0–1.16 Å after the initial step of refinement calculated at -2.5σ is shown with superimposed coordinates from the initial model. The negative density clearly indicates the presence of the smaller side chain (*i.e.* Leu) at position 112.

two residues, the salt bridge cannot be formed. The L3,4 loop in both D39A and R112L is thus shifted away in position from β8: by 1.2 Å in C^{α} positions for R112L and 0.5 Å for D39A (Fig. 3*b*). The overall conformation of the L3,4 loop remains unchanged and is probably dictated by the Pro-Gly sequence, which induces rigidity to the loop. The loop is shifted (rotated) along an axis defined by two anchoring points (the C^{α} atoms of residues 35 and 45) at the termini of the loop.

Upon binding of BNA, the L3,4 loop in both mutant structures is shifted back to a position similar to that observed for the AVR4–BNA complex (Fig. 3*c*). The shift is induced and stabilized by a specific interaction of the BNA amide O atom with the main-chain amide N atom of residue 39 (not shown). Accordingly, the conformation of the biotin moiety of BNA remains unchanged (Fig. 3*b*). In the D39A mutant, the hydrogen-bond interaction with Lys109 from the adjacent monomer is absent. The Arg112 side chain maintains a single conformation and forms a hydrogen-bond interaction with one of the BNA nitro O atoms (2.74 Å; Fig. 3*b*) as opposed to the alternate conformation observed in the AVR4–BNA structure (Prizant *et al.*, 2006). The conformation of the side chain Arg112 is also stabilized by a hydrogen-bond interaction between N^{ε} and the main-chain carbonyl O atom of Lys109 from the adjacent monomer.

In the various mutants, the position of the *p*-nitroanilide ring alters as a function of the size, reactivity and conformation of residue 112. Thus, in the structure of the R112L mutant the shorter and less bulky leucine side chain permits a shift of the *p*-nitroanilide moiety of BNA towards Leu112 and thus fails to form polar interactions with Asp39 from the L3,4 loop (Fig. 3*b*). As in wild-type AVR4, Asp39 from the L3,4 loop forms a polar interaction with Lys109 from the adjacent monomer. The lack of the crucial residue (Arg112) and the subtle change in the conformation of the *p*-nitroanilide group are likely to account for the difference in hydrolytic potential.

4. Discussion

In previous work, we noted a surprising peripheral difference between the highly similar egg-white protein avidin and its bacterial relative streptavidin. The observed pseudo-catalytic properties of avidin towards the BNP active ester contrasted sharply with the protective features of streptavidin. This diametrically opposed activity in the two homologous proteins spawned a series of studies designed to reveal the molecular basis for this unusual phenomenon. More recently, the discovery that the avidin-related protein AVR4 exhibits an even more dramatic pseudo-catalytic activity provided a new dimension to these studies. In addition to a superficial understanding of this phenomenon, the subtle differences in the enhanced hydrolytic

activity exhibited by avidin and AVR4 may provide insight into the initial stages of catalysis. As a consequence, we may be able to design avidin with a hydrolytic switch and/or with a defined reaction turnover, thus generating a true catalyst.

In both the apo and biotin-complexed forms of AVR4 there is a salt bridge between Asp39 from the L3,4 loop and Arg112 from β8 (Fig. 3*a*; Eisenberg-Domovich *et al.*, 2005). When AVR4 binds BNA, the salt-bridge interaction is disrupted and the two charged residues form a sandwich around the *p*-nitroanilide group (Prizant *et al.*, 2006). A similar disruption of the salt-bridge interaction is likely to occur when AVR4 binds other biotin derivatives or conjugates.

In addition, the two charged residues in AVR4 form polar interactions with the *p*-nitroanilide group. It has previously been shown that one of the significant factors that promotes BNP hydrolysis is its direct interaction with charged residues of the given avidin. Even though Asp39 and Arg112 of AVR4 are not directly involved in the cleavage of the ester bond, they may exert an effect on the BNP ligand that promotes catalysis by polarizing the relevant bond. Arg112 has already been suggested to be of high importance in promoting the leaving-group properties of the *p*-nitrophenyl group by withdrawing electrons from the system. Asp39 also forms a polar interaction with the nitro group, but its role in promoting BNP hydrolysis is less obvious. Based on these observations, we designed the R112L and D39A mutants of AVR4 in order to examine how each mutation affects its pseudo-enzymatic properties.

The results of the hydrolytic assay emphasize that Asp39 in AVR4, although interacting with the pseudo-substrate (and probably also affecting the binding of pseudo-substrate), does not appear to have a defined role in the enhancement of BNP hydrolysis (Fig. 1). The crystal structure of the AVR4(D39A) mutant indicates that the direct interaction between BNA and Arg112 is conserved (Fig. 3*c*) and the absence of the interaction with Asp39 does not influence the hydrolytic activity. On the other hand, these results clearly substantiate the role of Arg112 in enhancing the hydrolytic reaction (Fig. 1). The interaction of Arg112 with the nitro group of BNP probably increases the electron-withdrawing properties, thus increasing the leaving-group propensity of *p*-nitrophenol. The crystal structure of the AVR4(R112L) mutant demonstrates that the absence of the Arg–ligand interaction results in decreased hydrolytic activity (Fig. 3*c*). In the model of the AVR4(R112L)–BNA complex, the observed shift of the *p*-nitroanilide group of BNA towards Leu112 relative to its conformation in the wild-type and D39A-mutant models could also affect the activity.

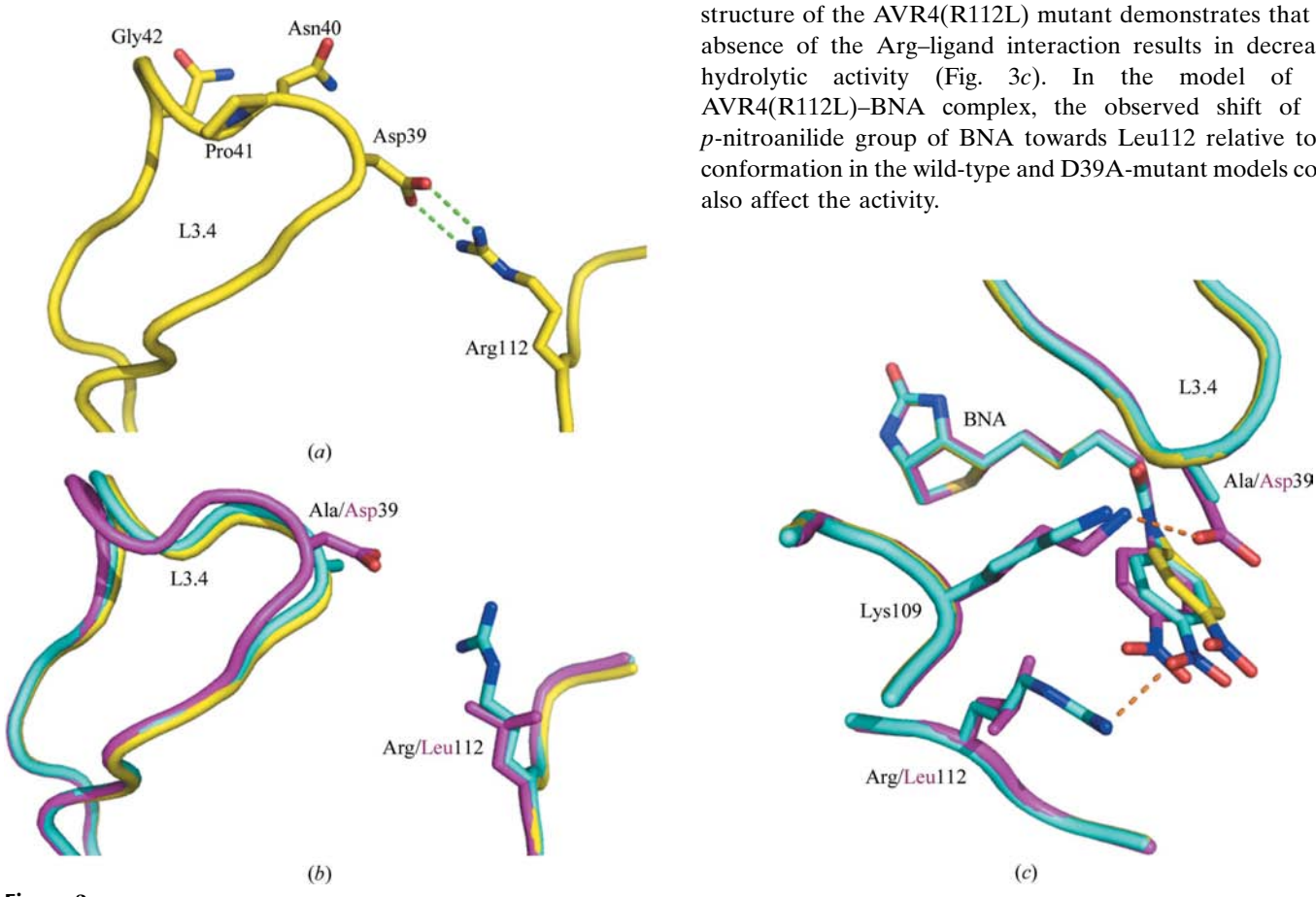

Figure 3
Structure models. (*a*) The salt-bridge interaction between Asp39 from the L3,4 loop and Arg112 from β8 in the wild-type apo AVR4 structure (PBD code 1y53). (*b*) In the apo models of the D39A (cyan) and R112L (magenta) mutants, the L3,4 loop is shifted away from its original position in wild-type AVR4 (yellow). Owing to the mutations, the salt-bridge interaction is eliminated, thus imparting flexibility to the L3,4 loop, although its overall conformation is maintained. (*c*) Upon BNA binding, the L3,4 loop in the two mutant structures attains the same position as observed in the wild-type AVR4. The conformation of the *p*-nitroanilide ring of BNA undergoes a shift from its original position in the wild-type model in the direction of residue 112. In the D39A mutant, the shift can be attributed to the lack of hydrogen-bond interactions (cyan), whereas in the R112L mutant the *p*-nitroanilide ring occupies part of the extra space afforded by the smaller residue at position 112 (magenta). All cartoons were produced using *PyMOL* (DeLano, 2002).

An even more crucial factor that defines the pseudo-catalytic activity of the avidins is the availability of the ester bond of the ligand to solvent, which is determined by the conformation of the L3,4 loop. As demonstrated previously for the avidins, ester hydrolysis is initiated by nucleophilic attack on the carbonyl C atom by hydroxyl ions in the solvent and not by an inherent protein-borne nucleophile. However, the availability of the ester bond to solvent is not the entire story. The efficiency of the hydrolytic reaction is actually a function of how the ester bond is displayed to the solvent. In wild-type avidin, the disordered conformation of the L3,4 loop allows flexibility in the position of the ester bond of the ligand. In contrast, the rigid conformation of the L3,4 loop in AVR4 allows presentation of the ester bond to the solvent in a single fixed conformation that is primed for nucleophilic attack.

Based on this premise, we have designed a modified avidin, avidin(L3,4-AVR4), in which the L3,4 loop was grafted from AVR4 into avidin. The resultant loop exchange served to increase the hydrolytic activity of avidin dramatically. Such an approach was also proved to be successful by converting streptavidin from a protector to an enhancer of BNP hydrolysis (Pazy, Eisenberg-Domovich *et al.*, 2003). These results substantiate the significance of the L3,4 loop conformation to the hydrolytic activity of the avidins and support recent findings (Tawfik, 2006) in which the replacement of several active-site loops in an enzyme led to a new enzymatic function.

In conclusion, in this study we have determined a defining characteristic, the critical conformation of the L3,4 loop, in the continuously developing story of the mechanism of BNP hydrolysis or pseudo-catalytic activity by the avidins. This artificial pseudo-enzyme system may be useful for studying enzyme action in general owing to its lack of turnover, which provides an intriguing opportunity to address experimentally the nature of a 'transition state' and the relative plasticity of a protein and its ligand. In addition, the observed pseudo-catalytic activity can be used to address other mechanistic features that may bear general relevance to enzymatic activity.

We thank the staff of the European Synchrotron Radiation Facility (ESRF), Grenoble, France for their assistance in maintaining and upgrading the MX beamlines in an exquisite state.

References

Amemiya, Y., Tanaka, T., Yoza, B. & Matsunaga, T. (2005). *J. Biotechnol.* **120**, 308–314.

Berman, H. M. *et al.* (2002). *Acta Cryst.* D**58**, 899–907.

Chilkoti, A., Tan, P. H. & Stayton, P. S. (1995). *Proc. Natl Acad. Sci. USA*, **92**, 1754–1758.

DeLano, W. L. (2002). *The PyMol Molecular Graphics System.* http://www.pymol.org.

Eisenberg-Domovich, Y., Hytönen, V. P., Wilchek, M., Bayer, E. A., Kulomaa, M. S. & Livnah, O. (2005). *Acta Cryst.* D**61**, 528–538.

Eisenberg-Domovich, Y., Pazy, Y., Nir, O., Raboy, B., Bayer, E. A., Wilchek, M. & Livnah, O. (2004). *Proc. Natl Acad. Sci. USA*, **101**, 5916–5921.

Green, N. M. (1975). *Adv. Protein Chem.* **29**, 85–133.

Green, N. M. (1990). *Methods Enzymol.* **184**, 51–67.

Grubmuller, H. (2005). *Methods Mol. Biol.* **305**, 493–515.

Hendrickson, W. A., Pahler, A., Smith, J. L., Satow, Y., Merritt, E. A. & Phizackerley, R. P. (1989). *Proc. Natl Acad. Sci. USA*, **86**, 2190–2194.

Huberman, T., Eisenberg-Domovich, Y., Gitlin, G., Kulik, T., Bayer, E. A., Wilchek, M. & Livnah, O. (2001). *J. Biol. Chem.* **276**, 32031–32039.

Hytönen, V. P., Laitinen, O. H., Airenne, T. T., Kidron, H., Meltola, N. J., Porkka, E., Hörhä, J., Paldanius, T., Määttä, J. A., Nordlund, H. R., Johnson, M. S., Salminen, T. A., Airenne, K. J., Ylä-Herttuala, S. & Kulomaa, M. S. (2004). *Biochem. J.* **384**, 385–390.

Hytönen, V. P., Laitinen, O. H., Grapputo, A., Kettunen, A., Savolainen, J., Kalkkinen, N., Marttila, A. T., Nordlund, H. R., Nyholm, T. K., Paganelli, G. & Kulomaa, M. S. (2003). *Biochem. J.* **372**, 219–225.

Hytönen, V. P., Maatta, J. A., Nyholm, T. K., Livnah, O., Eisenberg-Domovich, Y., Hyre, D., Nordlund, H. R., Horha, J., Niskanen, E. A., Paldanius, T., Kulomaa, T., Porkka, E. J., Stayton, P. S., Laitinen, O. H. & Kulomaa, M. S. (2005). *J. Biol. Chem.* **280**, 10228–10233.

Hytönen, V. P., Nyholm, T. K., Pentikainen, O. T., Vaarno, J., Porkka, E. J., Nordlund, H. R., Johnson, M. S., Slotte, J. P., Laitinen, O. H. & Kulomaa, M. S. (2004). *J. Biol. Chem.* **279**, 9337–9343.

Jones, T. A. & Kjeldgaard, M. (1997). *Methods Enzymol.* **277**, 173–208.

Keinanen, R. A., Wallen, M. J., Kristo, P. A., Laukkanen, M. O., Toimela, T. A., Helenius, M. A. & Kulomaa, M. S. (1994). *Eur. J. Biochem.* **220**, 615–621.

Kurzban, G. P., Bayer, E. A., Wilchek, M. & Horowitz, P. M. (1991). *J. Biol. Chem.* **266**, 14470–14477.

Laitinen, O. H., Airenne, K. J., Hytonen, V. P., Peltomaa, E., Mahonen, A. J., Wirth, T., Lind, M. M., Makela, K. A., Toivanen, P. I., Schenkwein, D., Heikura, T., Nordlund, H. R., Kulomaa, M. S. & Yla-Herttuala, S. (2005). *Nucleic Acids Res.* **33**, e42.

Laitinen, O. H., Hytonen, V. P., Ahlroth, M. K., Pentikainen, O. T., Gallagher, C., Nordlund, H. R., Ovod, V., Marttila, A. T., Porkka, E., Heino, S., Johnson, M. S., Airenne, K. J. & Kulomaa, M. S. (2002). *Biochem. J.* **363**, 609–617.

Lamzin, V. S. & Wilson, K. S. (1993). *Acta Cryst.* D**49**, 129–147.

Livnah, O., Bayer, E. A., Wilchek, M. & Sussman, J. L. (1993). *Proc. Natl Acad. Sci. USA*, **90**, 5076–5080.

Murshudov, G. N., Vagin, A. A. & Dodson, E. J. (1997). *Acta Cryst.* D**53**, 240–255.

Otwinowski, Z. & Minor, W. (1997). *Methods Enzymol.* **276**, 307–326.

Pazy, Y., Eisenberg-Domovich, Y., Laitinen, O. H., Kulomaa, M. S., Bayer, E. A., Wilchek, M. & Livnah, O. (2003). *J. Bacteriol.* **185**, 4050–4056.

Pazy, Y., Kulik, T., Bayer, E. A., Wilchek, M. & Livnah, O. (2002). *J. Biol. Chem.* **277**, 30892–30900.

Pazy, Y., Raboy, B., Matto, M., Bayer, E. A., Wilchek, M. & Livnah, O. (2003). *J. Biol. Chem.* **278**, 7131–7134.

Potterton, E., Briggs, P., Turkenburg, M. & Dodson, E. (2003). *Acta Cryst.* D**59**, 1131–1137.

Prizant, M., Eisenberg-Domovich, Y., Hytonen, V. P., Kulomaa, M. S., Wilchek, M., Bayer, E. A. & Livnah, O. (2006). *J. Mol. Biol.* **358**, 754–763.

Sano, T. & Cantor, C. R. (1995). *Proc. Natl Acad. Sci. USA*, **92**, 3180–3184.

Stura, E. A. & Wilson, I. A. (1991). *J. Cryst. Growth*, **110**, 270–282.

Tawfik, D. S. (2006). *Science*, **311**, 475–476.

Wilchek, M. & Bayer, E. A. (1990). *Methods Enzymol.* **184**, 14–45.